

Technical Comment

Comment on “Sensitivity of seafloor bathymetry to climate-driven fluctuations in mid-ocean ridge magma supply”

Peter Huybers^{1*}, Charles Langmuir¹, Richard Katz³, David Ferguson¹, Cristian Proistosescu¹, Suzanne Carbotte²

¹Harvard University, ²Lamont-Doherty Earth Observatory, ³University of Oxford,

*To whom correspondence should be addressed. E-mail: phuybers@fas.harvard.edu

Abstract

Olive et al. (Reports, 16 October 2015, p. 310) argue that order 10% fluctuations in melt supply do not produce appreciable changes in ocean ridge bathymetry on time scales less than 10^5 years, and thus cannot reflect sea-level forcing. Spectral analysis of bathymetry in a region they highlight as being fault controlled also shows strong evidence for a signal from sea level variation.

Olive et al.¹ argue that abyssal hills on the seafloor do not contain appreciable contributions from the influence of sea level change on magma production at ocean ridges. This hypothesis was originally suggested by Huybers and Langmuir (2009)² and further elaborated and supported by mantle melt modeling and observations on the Australian-Antarctic ridge by Crowley et al. (2015)³.

Olive et al. consider separately intrusive and extrusive magma additions, but claim that bathymetric variations from both of these can only result in topographic variations of less than 85m amplitude for magma volumes that fluctuate at Milankovitch periods (see their Figure 2). Constructional topography of far greater extent, however, is common at slow and intermediate spreading ridges. A split seamount and the pairs of symmetric ridges at the intermediate spreading Endeavor segment in the northeast Pacific are both demonstrably constructional features created on axis and preserved off-axis⁴. The common axial volcanic ridges at slowly spreading ridges⁵, where elastic thickness is greatest, are also constructional features, tens of km long with vertical relief of several hundred meters and a cross sectional scale that can be less than 2km. Lucky Strike seamount rises a km above the axis of the slow-spreading Mid-Atlantic ridge⁶. The Southeast Indian Ridge^{7,8} and Galapagos Spreading Center^{9,10}, which have near constant spreading rates but variable magma supply along axis, show marked differences in axial topography in response to melt flux variations of similar magnitudes to those proposed by Crowley et al. Despite the inferences Olive et al. draw from their models, seafloor topography of many hundreds of meters that reflects changes in magmatic budget is a common feature of ocean ridges.

A closer examination of the Chile Rise segment used by Olive et al. offers evidence for the conclusions of Crowley et al. Large offset faults are apparent in the bathymetry, but there are also smaller linear ridges and numerous volcanic cones with relief of about 100 m, particularly at the edges of the segment (see Olive et al.'s Figure 1). Accordingly, we

analyze a transect near 39° South from cruise PANR04MV near the northern edge of the Chile Rise segment. Crustal age is estimated using a Brunhes-Matuyama magnetic reversal of 780 ky. Spectral analysis is carried out following the multi-taper methodology of Crowley et al., wherein statistical significance is judged at the 95% confidence level relative to a chi-square null distribution¹¹. Significant spectral peaks occur at the Milankovitch periods of 100 ky, 41 ky, and near the 23 ky periods, matching those found in sea level variability (Figure 1), and in agreement with the independent analysis of the Australian-Antarctica Ridge by Crowley et al. Other transects from the Chile Rise show similar behavior, especially near the edges of the segment, but not as clearly. Topography associated with short term fluctuations in magma supply may be better preserved near the ends of ridge segments on the Chile Rise where crustal magma reservoirs may be present only during periods of magma excess.

Olive et al. argue that the appearance of 100 ky variability could be an emergent timescale associated with extensional faulting, and that spectral peaks at higher frequencies could result from overtones of 100 ky fault spacing. Two further observations, however, indicate that the Chile Rise bathymetry is not just faulting masquerading as Milankovitch. First, bathymetry variations prior to 700 ky are characterized by smaller amplitude oscillations and a 41 ky timescale, consistent with the dominant 41 ky obliquity period variability found in Early Pleistocene sea level. Second, examination of the temporal variability shows high-frequency variations in bathymetry similar in structure to sea level estimates and distinct from the abrupt changes that give rise to strong overtones in Olive et al.'s simulations (see Figure 1).

Numerous processes missing from Olive et al.'s models might explain their inability to produce significant sealevel-induced bathymetry emerging from observations. For example, dike induced faulting¹² and eruption dynamics including effusion rates that govern how lavas accumulate on the seafloor¹³ are not considered. Rather than new pulses of magma effectively mixed across a 1 km wide magma storage zone as modeled by Olive et al., local crustal magma sills could wax and wane as magma supply varies¹⁴, and large magma pulses could migrate vertically without mixing in a broader crustal reservoir. Although we agree that Crowley et al.'s approach of predicting bathymetric variations assuming local isostasy is probably too simple, it appears that Olive et al.'s models also omit important processes.

Olive et al. dismiss the importance of volcanic construction on the basis that it is "unlikely to strongly overprint the tectonic fabric of the seafloor, which typically consists of fault scarps greater than 200 m at slow and intermediate-spreading ridges". Normal faults do of course contribute importantly to the fabric of the sea floor, but do not preclude the presence of additional structure. We suggest the need for a more resolved approach than the historical characterization of abyssal hills using a single wavelength^{15,16}. The approach in Crowley et al. of pre-whitening the spectral estimate has the effect of emphasizing higher-frequency variability and leads to the identification of multiple relevant time-scales, namely those associated with 100 ky glacial, 41 ky obliquity, and 23 ky precession variations. This more detailed seafloor relief is an opportunity to better understand the relative contributions of volcanic and tectonic processes at mid-ocean ridges.

References:

1. Olive, J. A., Behn, M. D., Ito, G., Buck, W. R., Escartín, J., & Howell, S. (2015). Sensitivity of seafloor bathymetry to climate-driven fluctuations in mid-ocean ridge magma supply. *Science*, 350(6258), 310-313.
2. Huybers, P., & Langmuir, C.H., (2009). Feedback between deglaciation, volcanism, and atmospheric CO₂. *Earth and Planetary Science Letters*, 286(3-4), 479–491. <http://doi.org/10.1016/j.epsl.2009.07.014>
3. Crowley, J. W., Katz, R. F., Huybers, P., Langmuir, C. H., & Park, S. H. (2015). Glacial cycles drive variations in the production of oceanic crust. *Science*, 347(6227), 1237-1240.
4. Clague, D. A., B. M. Dreyer, J. B. Paduan, J. F. Martin, D. W. Caress, J. B. Gill, D. S. Kelley, H. Thomas, R. A. Portner, J. R. Delaney, T. P. Guilderson, and M. L. McGann (2014), Eruptive and tectonic history of the Endeavour Segment, Juan de Fuca Ridge, based on AUV mapping data and lava flow ages, *Geochem. Geophys. Geosyst.*, 15, 3364–3391, doi:10.1002/2014GC005415
5. Searle, R. C., Murton, B. J., Achenbach, K., LeBas, T., Tivey, M., Yeo, I., Cormier, M.H., Carlut, J., Ferreira, P., Mallows, C., Morris, K., Schroth, N., van Calsteren, P., Waters, C. (2010). Structure and development of an axial volcanic ridge: Mid-Atlantic Ridge, 45 N. *Earth and Planetary Science Letters*, 299(1), 228-241.
6. Detrick, R.S. D. Needham and V. Renard (1995) Gravity anomalies and crustal thickness variations along the mid-Atlantic Ridge from 33°N to 40°N. *J. Geophys. Res.* 100, 3767-3787.
7. Sempéré, J. C., & Cochran, J. R. (1997). The Southeast Indian Ridge between 88 E and 118 E: Variations in crustal accretion at constant spreading rate. *Journal of Geophysical Research*
8. Holmes, R. C., Tolstoy, M., Cochran, J. R., & Floyd, J. S. (2008). Crustal thickness variations along the Southeast Indian Ridge (100–116 E) from 2-D body wave tomography. *Geochemistry, Geophysics, Geosystems*, 9(12).
9. Sinton, J., Detrick, R., Canales, J. P., Ito, G., & Behn, M. (2003). Morphology and segmentation of the western Galápagos Spreading Center, 90.5–98 W: Plume-ridge interaction at an intermediate spreading ridge. *Geochemistry, Geophysics, Geosystems*, 4(12).
10. Canales, J. P., Ito, G., Detrick, R. S., & Sinton, J. (2002). Crustal thickness along the western Galápagos Spreading Center and the compensation of the Galápagos hotspot swell. *Earth and Planetary Science Letters*, 203(1), 311-327.
11. Percival, D. B., & Walden, A. T. (1993). *Spectral analysis for physical applications*. Cambridge University Press.
12. Carbotte, S. M., Detrick, R. S., Harding, A., Canales, J. P., Babcock, J., Kent, G., ... & Diebold, J. (2006). Rift topography linked to magmatism at the intermediate spreading Juan de Fuca Ridge. *Geology*, 34(3), 209-212.
13. Perfit, M. R., & Chadwick, W. W. (1998). Magmatism at mid-ocean ridges: Constraints from volcanological and geochemical investigations. *Geophysical Monograph-American Geophysical Union*, 106, 59-116. : *Solid Earth (1978–2012)*, 102(B7), 15489-15505.
14. Sinton, J. M., & Detrick, R. S. (1992). Mid-ocean ridge magma chambers. *J. geophys. Res.*, 97(197-288), 216.
15. Goff, J. A. (1991). A global and regional stochastic analysis of near-ridge abyssal hill morphology. *Journal of Geophysical Research: Solid Earth (1978–2012)*, 96(B13), 21713-21737.
16. Goff, J. A. (2015). Comment on “Glacial cycles drive variations in the production of oceanic crust”. *Science*, 349(6252), 1065-1065.
17. Siddall, M., Hönisch, B., Waelbroeck, C., & Huybers, P. (2010). Changes in deep Pacific temperature during the mid-Pleistocene transition and Quaternary. *Quaternary Science Reviews*, 29(1), 170-18.

Acknowledgements: This work was funded by NSF award 1338832.

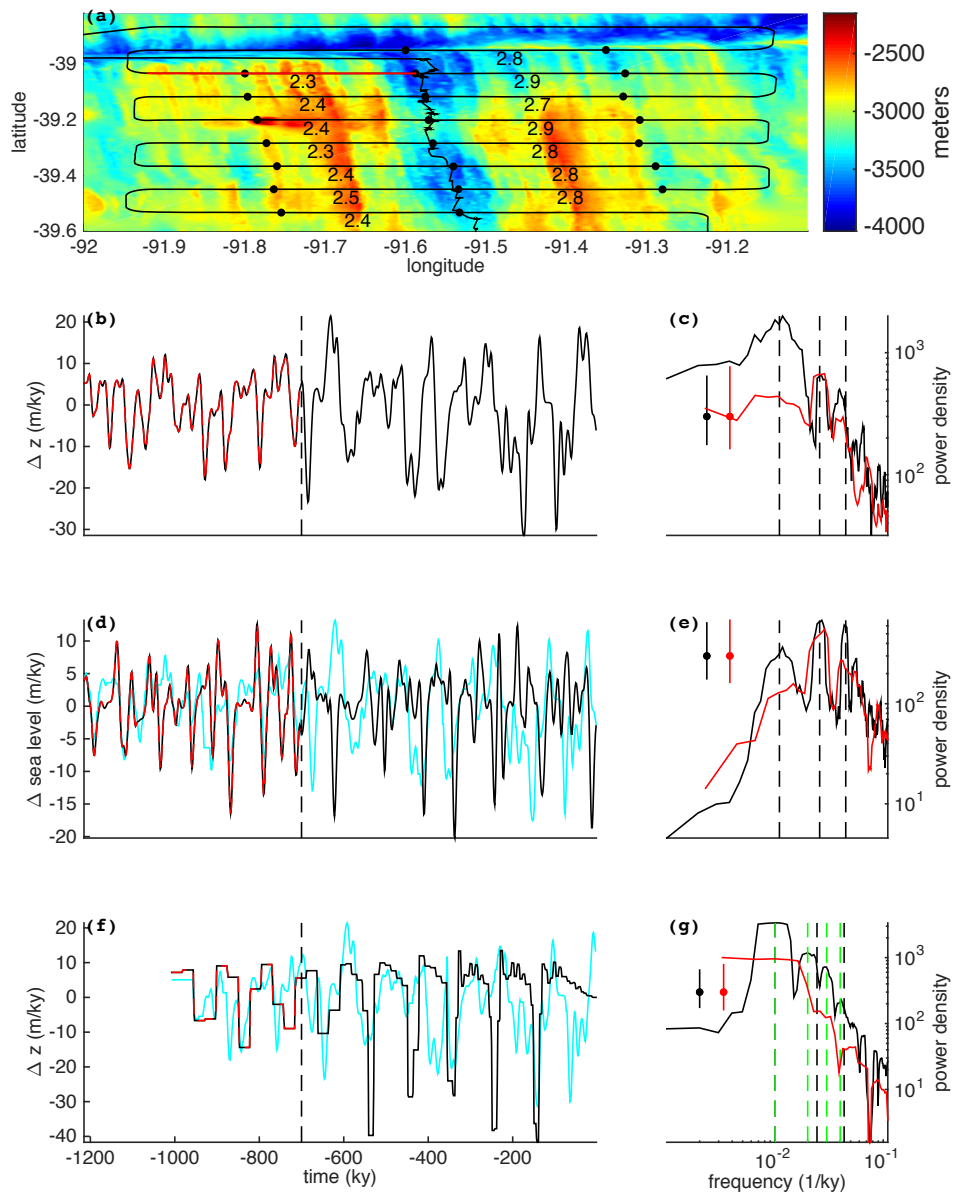


Figure 1. Bathymetry from the Chile Rise. (a) Map of bathymetry (coloring), the track from cruise PANR04MV (black line), Brunhes-Matuyama reversals from magnetics and visually identified ridge center (dots), inferred spreading rates (numbers in cm/yr), and the transect that we focus on (thick red line). (b) Rate of change of the bolded bathymetry section, and (c) the associated spectral estimate (black) indicating peaks near the 1/100, 1/41, and 1/23 ky^{-1} Milankovitch bands (marked with vertical dashed lines). Spectral peaks are statistically significant when they rise above the background continuum by more than the 95th percentile (i.e., after aligning the dot on the black confidence bar with the spectral peak, the lower vertical bar does not reach the level of the background continuum). Note the use of logarithmic axes. Also shown is a spectral estimate for the time period between 1.2Ma and 0.7Ma during the '41 ky' world (red), where there is significant spectral energy at the 41 ky obliquity band (judged using the red vertical bar) but the other Milankovitch bands are diminished. (d, e) Analysis of sea level changes (ref. 17, note reversal of the y-axis) shows spectral peaks matching (c). A version of the bathymetry rates-of-change are also shown (cyan) after alignment with the sea level variations using a dynamic time warping algorithm and scaling to match variance. (f, g) The analysis is repeated using the faulting simulations from Olive15 with a 100ky time scale, but which obviously cannot reproduce the transition to 41 ky variability. Overtones of the 100ky time scale are indicated at 2/100, 3/100, and 4/100 ky^{-1} (green vertical dashed lines). An aligned version of the bathymetry data is also presented (cyan) that illustrates difference between the continuous high-frequency variability recorded in bathymetry and abrupt transitions in the fault simulation.